RESISTANCES OF A STAINLESS STEEL-CLAD REINFORCING BAR TO CHLORIDE-INDUCED CORROSION IN CONCRETE

Gerardo G. Clemeña, Ph.D.
Principal Research Scientist (Ret.)
Virginia Transportation Research Council
Charlottesville, VA 22903

SYNOPSIS

Corrosion of reinforcing bars has been a major factor in limiting the service life of many concrete bridges in the United States. To eliminate this problem and enable new concrete bridges to last a very long time, bars that are corrosion resistant, more durable than epoxy-coated bars, and yet economical are needed. For the purpose of finding such a bar, a recently introduced bar clad with stainless steel 316L was tested against a solid 316LN stainless steel bar and a carbon steel bar – in concrete blocks exposed to weekly cycles of ponding with a saturated salt solution and drying. To facilitate determination of the times-to-corrosion of these bars, their macrocell currents were monitored regularly for more than 3 years. The chloride corrosion thresholds of the bars were then estimated by laboratory analysis of the mean chloride contents of concrete samples taken from sixteen randomly selected concrete blocks, at different depths and salt exposure times. The results to date indicated that the clad bars have corrosion resistance that compared very favorably to that of the 316LN stainless steel bars.

Key Words: Concrete bridges, corrosion of reinforcing bars, stainless steel bars, carbon steel bars, clad steel bars.

INTRODUCTION

Prompted by constantly increasing construction costs and the constant lack of sufficient funds for maintenance of existing facilities and new construction, many state transportation agencies have recently adopted a longer design life of at least 75 years and 100 years for minor and major concrete bridges, respectively, without major repairs. Since chloride-induced corrosion of reinforcing bars has been a major cause of premature deterioration of many concrete bridges, to achieve these high service-life goals would require either major improvement to the

current epoxy-coated carbon steel bars (ECR) or development of new bars that are not only intrinsically more corrosion resistant but also reasonably affordable. The ability of bars made of certain austenitic stainless steels, which are intrinsically corrosion resistant, to withstand high concentrations of chlorides in concrete has been indicated in several investigations conducted since 1985.[1,2,3,4] These findings mean that concrete bridges built with any of these bars can last a long time, likely much longer than those built with ECRs. However, the average cost of in-place stainless steel bars is prohibitively high – more than 4 times that of ECRs.

Because of the need for an economical, corrosion-resistant bar, a 316L stainless steel–clad carbon steel bar was recently introduced from the U.K. Briefly, the production of the stainless steel-clad bars involved packing 316L stainless steel pipes with fine granules of carbon steel. These compacted composite pipes are then heated, in a furnace with a reducing environment, up to 1,250^{o}C (2,280^{o}F) and then hot rolled into clad bars of appropriate sizes. The stainless steel cladding is thereby intended to provide an extremely durable and yet economical protection to the less expensive carbon steel core.

Prompted by the prospect that these clad bars might significantly increase the service life of future concrete bridges in a cost-efficient manner, their resistances to corrosion in heavily salted concrete blocks were compared with that of a conventional carbon steel bar and an austenitic stainless steel bar. This paper discusses the results obtained so far. A similar comparison of the clad bars with the same stainless steel bars in simulated concrete pore solutions was reported earlier.[5]

EXPERIMENTAL PROCEDURE

The new clad bars were compared with a carbon steel bar (commonly called mild steel or black bar) and a 316LN austenitic stainless steel bar. Each of these two benchmark bars was meant to represent one different end of a corrosion-resistance spectrum – with poor corrosion resistance represented by the carbon steel bar, while excellent corrosion resistance represented by the 316LN bar. Both straight and U-bent forms of these bars were tested.

The thickness of the cladding on 32 pieces of clad bars was measured at two points (that represented a high and a low) at one end of each bar. The mean thickness of the stainless steel cladding on these bars was 1.08 mm (42 mil), with a standard deviation of 0.23 mm (9 mil). The minimum and maximum thickness was 0.44 mm (17 mil) and 1.43 mm (56 mil), respectively. For the purpose of assessing the effects of possible defects in the stainless steel cladding on the

carbon steel core, three 0.5-mm (0.020-in.) wide holes were intentionally drilled through the cladding in several clad bars, and an approximately 25-mm (1.0-in.) long and 1-mm (0.04-in) wide cut was made in several others to expose the carbon steel core before they were embedded in concrete.

Concrete Blocks and Their Accelerated Exposure to Salt

Several sets of concrete blocks (Figure 1) were constructed with the different bars embedded in the various combinations listed in Table 1. To assess the possible consequences of using one type of bar at the top mat and another at the bottom mat of a concrete bridge deck to reduce materials cost, some blocks were fabricated with one of the 316LN stainless steel bars or the clad bars at the top and carbon steel bars at the bottom.

A few days after the test concrete blocks were fabricated using the concrete mixture proportions given in Table 2, the form was removed from each block and a wooden dam was built on the top surface of the block. Then, all the concrete blocks were covered with sheets of heavy plastic and allowed to cure outdoors for approximately 4 weeks before the sides of each block were coated with a rapid-setting epoxy mix. Following this, all the test blocks were subjected to weekly cycles of ponding with a saturated solution of NaCl for 3 days and drying for 4 days.

Measurements Made on the Test Concrete Blocks

To define the initiation of corrosion on the different bars, the macrocell current flowing between bars in the top and bottom portions in each concrete block was measured weekly from the beginning of this ongoing investigation. This measurement was made using the voltage-drop method, whereby a 100-ohm resistor was connected between each top bar and the two bottom bars (as shown in Figure 1) and then the positive terminal of a high-impedance multimeter was connected to the end of the resistor that was connected to the top bar while the negative terminal was connected to the resistor's end connected to the bottom bars. In this manner, a negative voltage drop would correspond to a positive macrocell (galvanic) current, i.e., the top bars would be anodic in comparison to the bottom bars. Finally, the macrocell currents for all the top bars in the same subset of concrete blocks were averaged to yield the subset mean macrocell current for that weekly measurement.

To allow for estimation of the amount of chloride ions that penetrated the concrete blocks after various salt exposure cycles, the concentrations of the total (acid-soluble) chloride in 16

concrete blocks at depths ranging from 13 to 51 mm and exposure times ranging from 114 to 661 days were determined in accordance with ASTM C-1152.

RESULTS

Macrocell Currents

In a concrete bridge deck exposed to deicing salts, the top-mat reinforcing bars are typically the first ones to be exposed to moisture and chloride ions. This gives rise to concentration gradients of these substances (with respect to depth) and, therefore, electrochemical macrocells in the concrete, whereby the top bars become more anodic than the bottom ones, with current flowing between the two mats. It is believed that these macrocells are the major driving force of the all too familiar corrosion of the top reinforcing bars and the resulting delamination of the surrounding concrete. The design of the concrete blocks and the manner with which these were exposed to salt was intended to simulate this situation in real concrete bridge decks.

As basis for comparison, Figure 2 shows the weekly macrocell currents of the two subsets of concrete blocks that were reinforced with carbon steel bars, as these blocks were being subjected to outdoor weekly cycles of salt ponding and drying. As Figure 2 shows, the top bent carbon steel bars in both series of concrete blocks were initially passive, with mean macrocell currents of approximately 0.1 μA. This level of macrocell currents can be considered insignificant, since the accuracy of the measurement was estimated to be ± 0.2 μA. Then, beginning at days 90 to 95, the macrocell currents of both sets of concrete blocks began to exhibit rapid increases in the positive direction. This indicated that sufficient chloride ions had by then reached the top carbon steel bars to cause these to become anodic, with respect to the carbon steel bars at the bottom of those blocks.

During the 752 days of outdoor exposure, the maximum macrocell currents observed were 490.7 μA for one set and 534.9 μA for the other. (Table 3 lists the mean and maximum macrocell currents observed for these two sets of test blocks and all other sets of test blocks.) With differences of only 4%, the results presented in Figure 2 must be considered in excellent agreement.

Noteworthy in Figure 2 are the concurrent fluctuations in the macrocell currents of these two sets of test blocks, in response to changes in the outdoor exposure conditions (temperature

and rainfall) with seasons. In general, the peaks and the valleys in the two curves corresponded to the warmer spring and summer days and colder winter days, respectively.

Figure 3 shows the macrocell currents for the three subsets of concrete blocks containing 316LN bars, which are known for their excellent corrosion resistance. For those with 316LN in the top and bottom portions (i.e., blocks 316LN/316LN), their weekly macrocell currents even after 1,299 days (or 186 weekly cycles) of salt exposure were still practically indiscernible (even at an expanded scale of 40x) or insignificant, averaging only 0.0 μA at a standard deviation of ± 0.2 μA during that period, which indicates that the 316LN bars were still passive (Table 3). In addition, Figure 3 shows that after approximately 400 days, the concrete blocks with a combination of 316LN bars at the top and carbon steel bars at the bottom (i.e., the 316LN/CS and the Bent 316LN/CS blocks) began to exhibit negative macrocell currents. This indicated that sufficient chloride ions had reached the depth of the carbon steel bars, so that they became more anodic than the top 316 LN bars and were, therefore, corroding. As indicated in Table 3, the macrocell currents for these two subsets of blocks reached as much as - 9.0 to - 9.2 μA before measurements for these blocks were terminated at approximately 752 days due to cracking of some of the blocks at around the bottom carbon steel bars (see Figure 4).

The graphs for the new clad bars, which are shown in Figures 5, are essentially similar to those shown in Figure 3 for the 316LN bars. All of these graphs share two common characteristics. First, the lack of any significant macrocell current in the concrete blocks containing either 316LN or clad bars in both mats, even after 1,299 days of the salt exposure regime. This implies that the clad bars had, so far, exhibited the same good resistance to attack by chloride ions in concrete, as the solid 316LN bars had. Secondly, the appearances of undesirable negative macrocell currents (after 350 to 450 days) in the blocks wherein carbon steel bars were used in the bottom mat.

As additional (to the symptoms illustrated in Figure 4) proof that such negative macrocell currents mean that the bottom carbon steel bars were already corroding before the apparently more corrosion-resistant bars at the top were, four sets of those concrete blocks that showed negative currents were flipped upside down at approximately 270 days and the potentials and corrosion rates of the bottom carbon steel bars were measured – the latter using the linear polarization method, with the aid of a guard-ring electrode assembly, and assuming that the

surface area of the bar underneath the assembly is being uniformly polarized. The potentials of some of those bars were observed to be between -352 and –506 mV and the corrosion rates were as high as 1.8 to 37.3 $\mu A/cm^2$. Based on commonly accepted interpretation[6] that a measured corrosion rate of > 1.0 $\mu A/cm^2$ for conventional steel bars indicates presence of active corrosion, there is very little doubt that these bottom carbon steel bars were corroding.

The stainless steel clad bars with three holes drilled through the cladding had no significant macrocell current, even after 1,186 days of exposure (Figure 6). In contrast, the clad bars with a cut intentionally introduced through the cladding began to show measurable positive macrocell current at 392 days. However, the maximum macrocell current exhibited by these bars was only 10.5 μA on Day 456, which is comparatively less than the magnitudes of the currents observed on the carbon steel (Figure 2). Regardless, this likely indicates that the exposed carbon steel core underneath the cut had begun to corrode. It is worthwhile to continue observing these bars to determine whether this activity continues with time.

Concentration of the Chloride Ions in the Test Concrete Blocks

As shown in the preceding sections, the macrocell current and open-circuit potential of a metallic reinforcing bar reflected very much its corrosion state. Therefore, by weekly monitoring this simple electrochemical parameter, as the different bars were being regularly exposed to salt, the times-to-corrosion of these bars were effectively pinpointed. The times-to-corrosion of the different bars, which were estimated accordingly, are listed in Table 4. Although this time parameter is useful for comparing the bars, as later disccusions will show, a more useful one would be the amount of chloride ions that each type of bars was able to tolerate in the concrete, i.e., its chloride corrosion threshold.

To equate the estimated time-of-corrosion of each bar to its chloride corrosion threshold, the mean chloride concentrations in the concrete blocks at different depths were determined by analysis of the ground concrete samples extracted from 16 randomly selected test concrete blocks, after several different exposure times. From the best-fit curves for these several chloride ion distributions, the mean concentration of the chloride ions in the test blocks at the depth of of the top-mat bars – 33 mm – as a function of exposure time was derived (see Figure 7). This function, in turn, provided estimates of the chloride corrosion thresholds of the various bars, which are listed in Table 4.

DISCUSSION

Examination of all electrochemical data collected would indicate that both the macrocell current, in relation to exposure time, provide a definitive indication of when corrosion has begun on a particular type of bar. As clearly demonstrated in Figures 2, the onsets of corrosion in the carbon steel bars were all clearly characterized by a rise in the positive macrocell current in the concrete blocks. In contrast, the other bars, which were relatively more passive or corrosion resistant, exhibited no significant macrocell currents and considerably more stable potentials for much longer exposure times. Based on the exposure time at which each type of bars began to show significant changes in these two simple parameters, the time-to-corrosion of the different types of bars tested was estimated. In Table 4, the estimated relative times-to-corrosion and chloride corrosion thresholds of the different bars are tabulated in increasing order. It must be emphasized that the testing of those that have not corroded yet, is still in progress. Therefore, the relative rankings of these groups are yet to be determined.

This investigation estimated that the conventional carbon steel bars were able to withstand from 460 to 580 ppm of chloride in the concrete blocks, or 0.046% to 0.058% by weight of concrete, before corroding (Table 4). Previous investigators have reported threshold levels of 330 to 670 ppm.[7,8] Considering the differences in the manners with which the previous and the present investigators arrived at these threshold values, these values can be considered to be in good agreement.

Since the 316L-clad and the solid 316LN stainless steel bars were still passive after 1,299 days of weekly salt exposure, the threshold levels of these bars would be higher than 6,470 ppm or at least 11.2 to 14.2 times that of carbon steel. This is in agreement with earlier reports regarding specific stainless steels (such as 304, 316, and N33) that there were no significant differences in the resistances of these metallic bars to chloride ions and the chloride threshold levels of these bars ranged from more than 10 to 24 times that of carbon steel.[1,3,4,10]

The effect of cladding damage or defect on the corrosion resistance of stainless steel clad bars is an interesting issue. As indicated in the earlier discussion, when the defect or damage was a cut, of 25-mm (1.0-in.) long and 1-mm (0.04-in) wide, in each of the top clad bars, these bars began to show positive mean macrocell current between them top and the bottom clad bars and an abrupt shift toward electronegativity in their mean open-circuit potentials, at approximately 392 days. This signaled that corrosion was initiated on some of these clad bars with cuts at that

stage of the severe salt exposure. For visual confirmation, block CB (w/cut) –1 was autopsied to expose the two top clad bars with cuts (Figures 8 and 9). This revealed that bar 1A had no sign of corrosion at the cut, while bar 1B had two round corrosion areas – one of one end of the cut. Further examination of bar 1B revealed no further damage to the bar, and that the corrosion in both areas may have had subsided. The apparent absence of corrosion on bar 1A and the initiation and then probable subsidence of corrosion on bar 1B are strongly reflected on the macrocell currents of these individual bars (Figure 10). As shown, there was no significant macrocell current for bar 1A, even though it had a cut similar to that in bar 1B, which exibited macrocell current from approximately day 400. Another interesting aspect is the remaining two similar bars (2A and 2B) also exhibited significant but similarly small macrocell currents – with one bar starting at approximately 392 days. This means that 3 out of the 4 clad bars with a cut through the cladding have so far began to corrode.

In contrast, the absence of macrocell current for the entire 1,299 days of testing of the clad bars with holes drilled through the cladding (Figure 9) suggested no corrosion yet on these bars. Similar autopsy of a concrete block with two of these bars confiemed no sign of corrosion around each of the holes (Figure 11). All these results certainly pointed toward a possible influence of size of cladding defects on loss of protection for the carbon steel core, if any. The cuts introduced on some of the clad bars in this investigation were probably unrealistic. Although it is expected that the stainless steel cladding would be very resistant to damage by impact, abrasion, or penetration, it is conceivable that cladding “breaks” can occur if sections of clad bars with insufficient cladding are bent. In that case, what is the minimum of size of possible defects beyond which loss of protection for the core would be significant?

The results on the clad bars with the cuts raise an interesting question: Why didn't the area of carbon steel core exposed directly to the cement paste (and, therefore, chloride ions), through the cut in the cladding, behaved like a conventional carbon steel bar, instead of having an effective chloride threshold that is 6.5 to 8.5 times higher (see Table 4)?

Finally, the authors would like to caution that some of the chloride corrosion threshold values presented may differ from those to be obtained by other investigations, due to differences in test designs and methodology used. However, if any, the differences should be slight – as in the case of the thresholds obtained in this investigation and those earlier ones for carbon steel bars. It must also be noted that, just as important as corrosion threshold is in influencing the

effective service life of a particular bar, so are the other aspects of bar corrosion: the corrosion propagation rate and characteristic, which are the foci of an ongoing investigation.[9] When used in conjunction with relevant factors such as expected salting rate, concrete mix design, concrete cover (over the bars), cost of bars, etc., information on these three aspects of bar corrosion should facilitate the design of future concrete structures that will meet any realistic combination of service-life and cost-effectiveness goals.

CONCLUSIONS

The macrocell current data presented have demonstrated beyond any doubt that this parameter, when monitored sufficiently frequent, is very useful for identifying the onset of corrosion in a metallic reinforcing bar.

Within their more than 3-year testing time frame, the defect-free clad bars have shown excellent corrosion resistance as the solid and costlier 316LN stainless steel bars —indicating that the stainless steel cladding is providing the intended protection for the carbon steel core. Depending on their size, defects in the cladding may negate this protection somewhat. However, there is evidence to show that corrosion on the core caused by cladding defect may be slow, in comparison to those on non-cladded carbon steel bars.

Last, the risk arising from the use of a combination of a more expensive corrosion-resistant bar in the top-mat reinforcement of a concrete bridge deck and the cheaper but corrosion-susceptible carbon steel bars in the bottom mat needs to be emphasized. Depending on the permeability of the concrete, sufficient chloride ions could reach the bottom carbon steel bars during the life of a structure to cause them to corrode before the more corrosion-resistant top bars – in which case, the consequential necessary repairs to the structure would be extremely more difficult and costly.

REFERENCES

1. Zoob, A. B., LeClaire, P. J., and Pfeifer, D. W., "Corrosion Tets on Reinforced Concrete With Solid Stainless Steel Reinforcing Bars for Joslyn Stainless Steels," Wiss, Janney, Elstner, Inc., Northbrook, Illinois, 1985.

2. McDonald, D. B., Pfeifer, D. W., and Blake, G. T., "The Corrosion Performance of Inorganic-, Ceramic-, and Metallic-Clad Reinforcing Bars and Solid Metallic Reinforcing Bars

in Accelerated Screening Tests," Report No. FHWA-RD-96-085. Federal Highway Administration, Washington, D.C., 1996.

3. Gu, P., Elliot, S., Beaudoin, J. J., and Arsenault, B., "Corrosion Resistance of Stainless Steel in Chloride Contaminated Concrete," *Cement and Concrete Research*, Vol. 26, No. 8, pp. 1151-1156, 1996.

4. McDonald, D. B., Pfeifer, D. W., and Sherman, M. R., "Corrosion Evaluation of Epoxy-Coated, Metallic-Clad and Solid Metallic Reinforcing Bars in Concrete," Report No. FHWA-RD-98-153. Federal Highway Administration, Washington, D.C., 1998.

5. Hurley, M. F., Scully, J. R., and Clemeña, G. G., "Selected Issues in Corrosion Resistance of Stainless Steel Clad Rebar," *Corrosion 2001*, National Association of Corrosion Engineers – International, Houston, Texas, 2001.

6. Broomfield, J. P., Rodriquez, J., Ortega, L. M., and Garcia, A. M., "Corrosion Rate Measurement and Life Prediction for Reinforced Concrete Structures," Proceedings of the Structural Faults and Repairs – 1993, Unversity of Edinburg, Scotland, Vol. 2, pp. 155-164., 1993.

7. Lewis, D. A., "Some Aspects of the Corrosion of Steel in Concrete," *Proceedings of the First International Congress on Metallic Corrosion*, London, pp. 547-555, 1962.

8. Pettersson, K., "Chloride Threshold Value and the Corrosion Rate in Reinforced Concrete," *Cement and Concrete Research*, Vol. 24, pp. 461-470, 1994.

9. Scully, J. R., and Clemeña, G. G., "Work Plan: Investigation of the Corrosion Propagation Characteristics of New Metallic Reinforcing Bars," Virginia Transportation Research Council, Charlottesville, Virginia, 2002.

10. Nurnberger, U., Beul, W., and Onuseit, G., "Corrosion Behavior of Welded Stainless Reinforcing Steel in Concrete." *Otto Graf Journal*, Vol. 4, pp. 225-259, 1993.

Table 1
TEST CONCRETE BLOCKS

Bar	Bar Combination		No. of Blocks	Block Designation
	Top Bars	Bottom Bars		
Carbon Steel	Straight Carbon Steel	Straight Carbon Steel	4	CS/CS
	Bent Carbon Steel	Straight Carbon Steel	8	Bent CS/CS (1)*
	Bent Carbon Steel	Straight Carbon Steel	4	Bent CS/CS (2)*
316LN	Straight 316LN	Straight 316LN	4	316LN/316LN
	Straight 316LN	Straight Carbon Steel	4	316LN/CS
	Bent 316LN	Straight Carbon Steel	8	Bent 316LN/CS
316L-Clad	Straight Clad Bar	Straight Clad Bar	4	CB/CB
	Straight Clad Bar (w/holes)	Straight Clad Bar	4	CB (w/holes)/CB
	Straight Clad Bar	Straight Carbon Steel	4	CB/CS
	Bent Clad Bar	Straight Carbon Steel	8	Bent CB/CS
	Bent Clad Bar (w/cut)	Straight Clad Bar	4	CB (w/cut)/CB

* Denotes either series-1 or -2 concrete blocks.

TABLE 2
CONCRETE MIXTURE USED FOR THE TEST BLOCKS

Water-cement ratio (*w/c*)	0.50
Cement (kg/m^3)	390
Coarse aggregates (kg/m^3)	1,059
Fine aggregates (kg/m^3)	828

Table 3
MACROCELL CURRENTS OBSERVED ON VARIOUS GROUPS OF TEST CONCRETE BLOCKS

Test Blocks	Macrocell Current (μA)		Total Exposure Time (day)
	Mean	Maximum	
			752
			735
316LN/316LN	0.0	0.4	1,299
316LN/CS	-0.9	-9.2	752
Bent 316LN/CS	-1.0	-9.0	752
			1,299
			1,299
			899
			752
			752

*The sign indicates the direction of current flow between the top and the bottom mats.

TABLE 4
ESTIMATED RELATIVE TIMES-TO-CORROSION AND CHLORIDE THRESHOLD CONCENTRATIONS FOR THE DIFFERENT BARS

Bar	Time-to-Corrosion (day)	Chloride Threshold (ppm)	Threshold Ratio
Carbon Steel	90 to 95	460 to 580	1.0
316L-Clad with Cut	392 to 413	3,770 to 3,890	6.5 to 8.5
316L-Clad with Holes	> 1,299	> 6,470	> 11.2 to 14.2
316L-Clad	> 1,299	> 6,470	> 11.2 to 14.2
316 LN	> 1,299	> 6,470	> 11.2 to 14.2

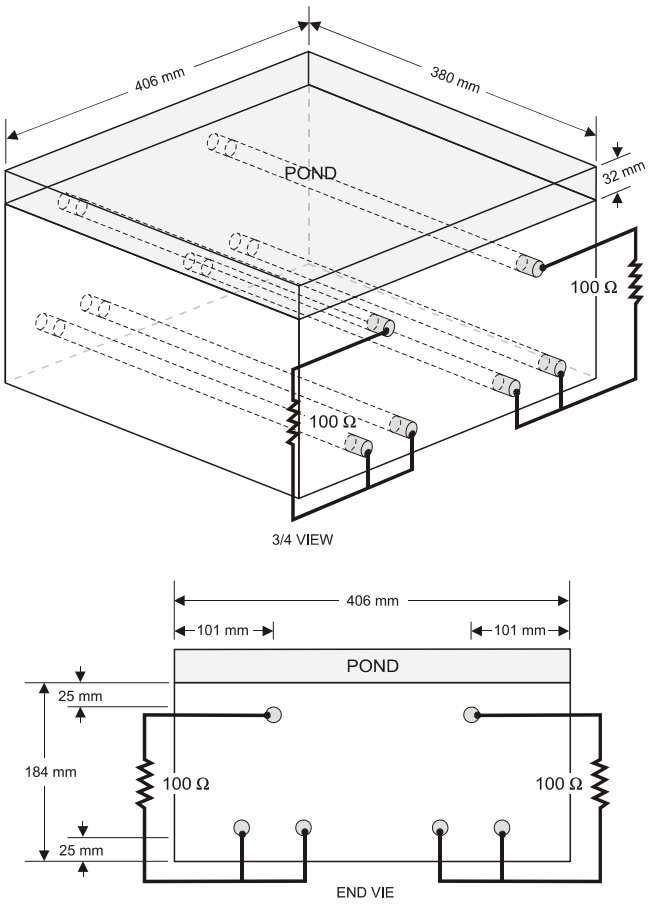

Figure 1. Test concrete blocks. The blocks had either straight or bent bars at the top, while all bottom bars were straight.

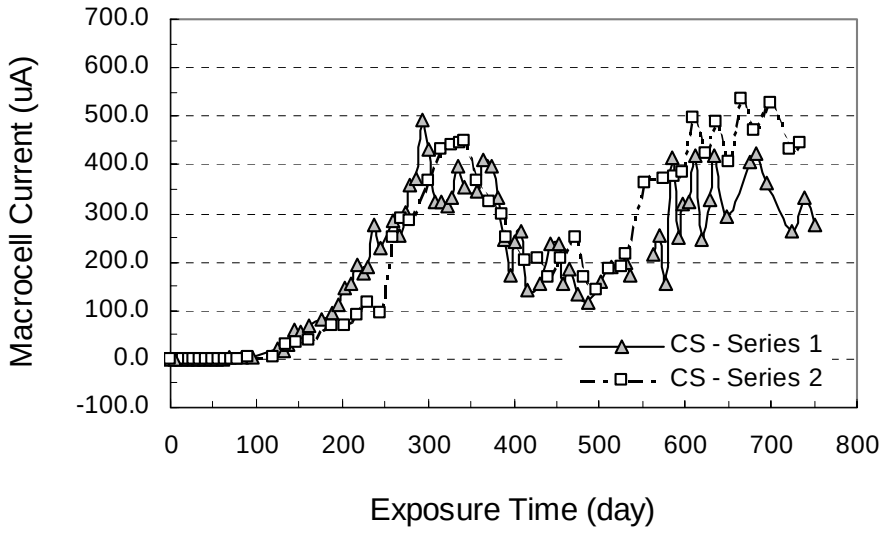

Figure 2. Macrocell current of the two sets of test concrete blocks with bent carbon steel bars at the top and straight carbon steel bars at the bottom portion of each block.

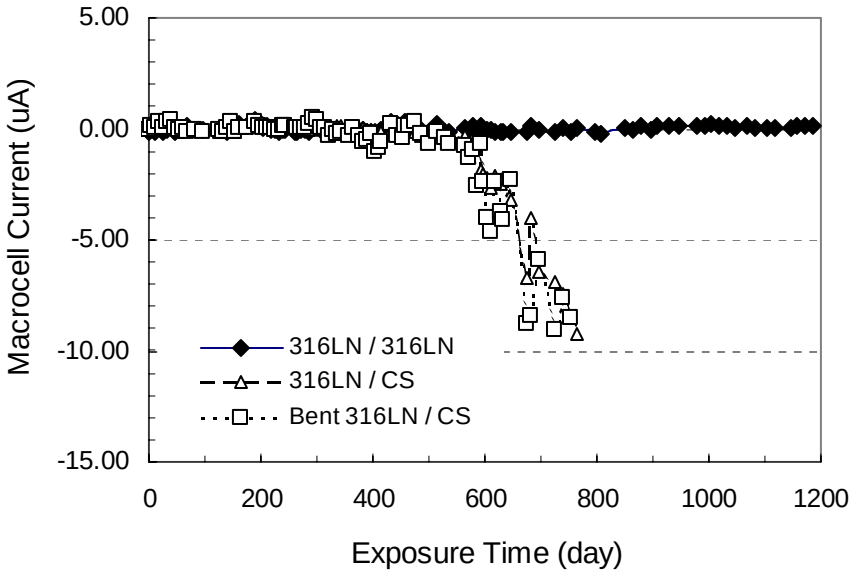

Figure 3. Macrocell current of test concrete blocks with 316LN stainless steel bars in various bar combinations described in Table 1.

Figure 4. Side view of a concrete block with 316LN bars at the top and carbon steel bars at the bottom.

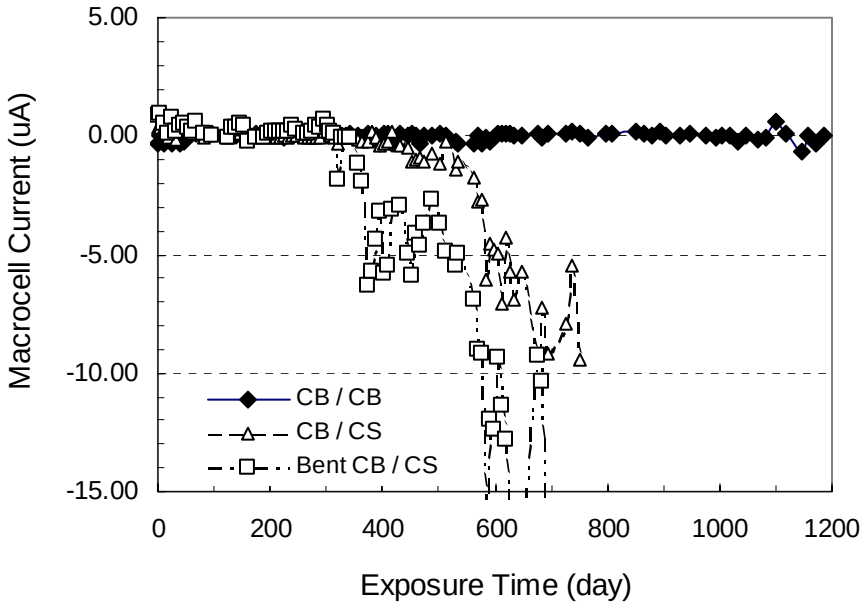

Figure 5. Macrocell current of test concrete blocks with 316L stainless steel-clad bars in various bar combinations.

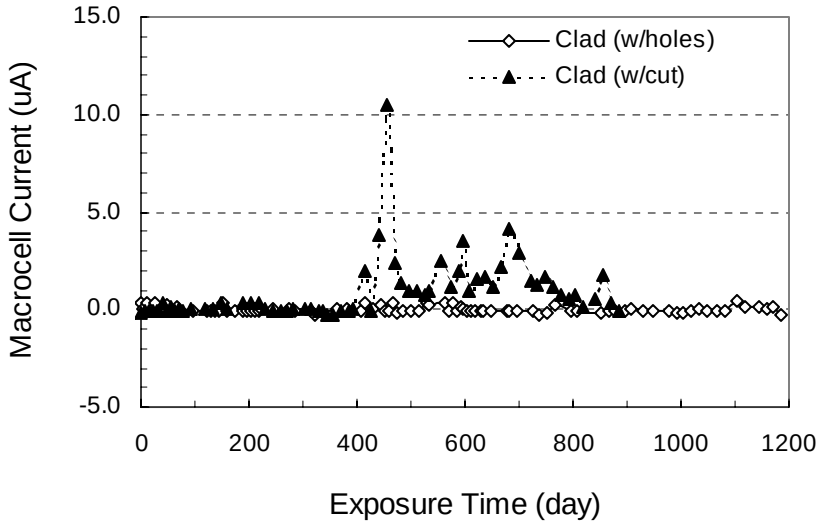

Figure 6. Macrocell currents of the concrete blocks with the clad bars with either drilled holes or a cut through the cladding.

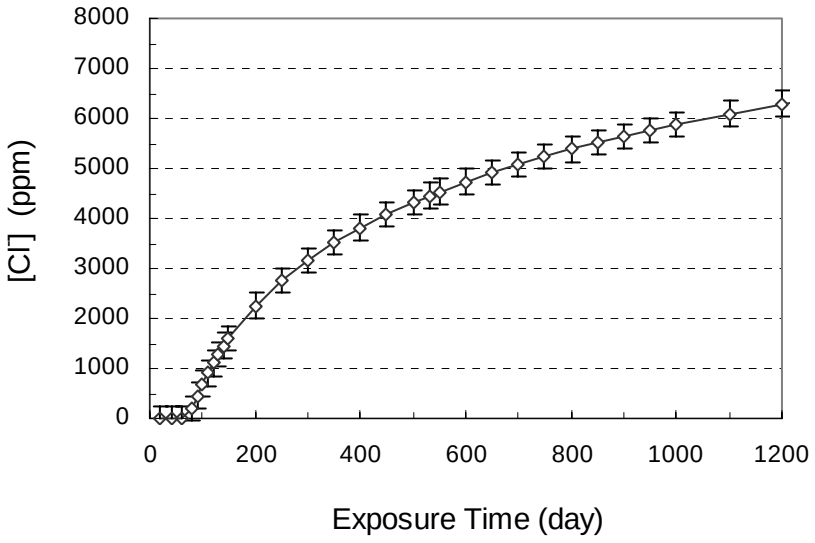

Figure 7. Estimated mean chloride concentrations in the concrete blocks, at the depth of top bars (33 mm), as a function of exposure time.

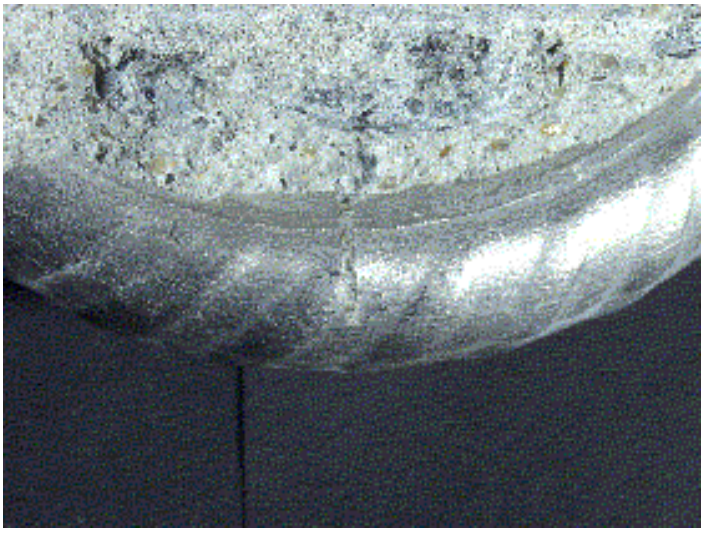

Figure 8. A clad bar with cut in the cladding (1A) recovered from a concrete block. Notice the absence of corrosion in the vicinity of the cut, which was completely filled with cement paste (center of photo).

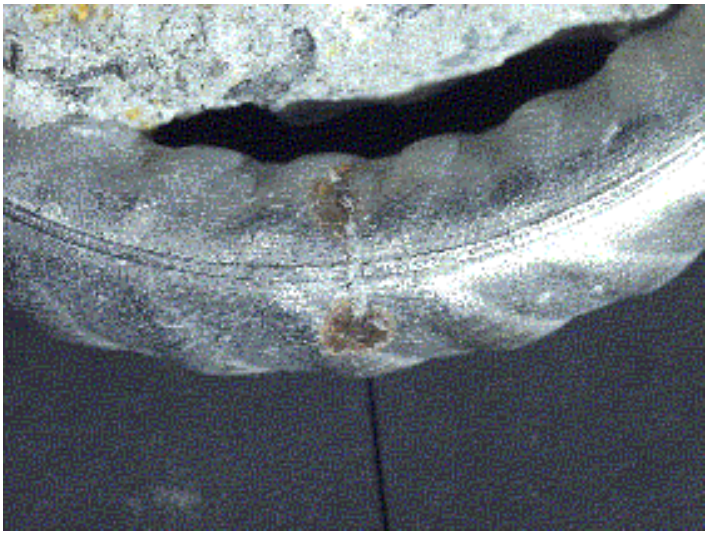

Figure 9. Another clad bar with cut in the cladding (1B) recovered from a concrete block. Notice the presence of two corrosion areas, which were 4 to 5 mm (0.16 to 0.20 in) wide, at the ends of the cut (center of photo). Notice that the cut was practically filled with cement paste**.**

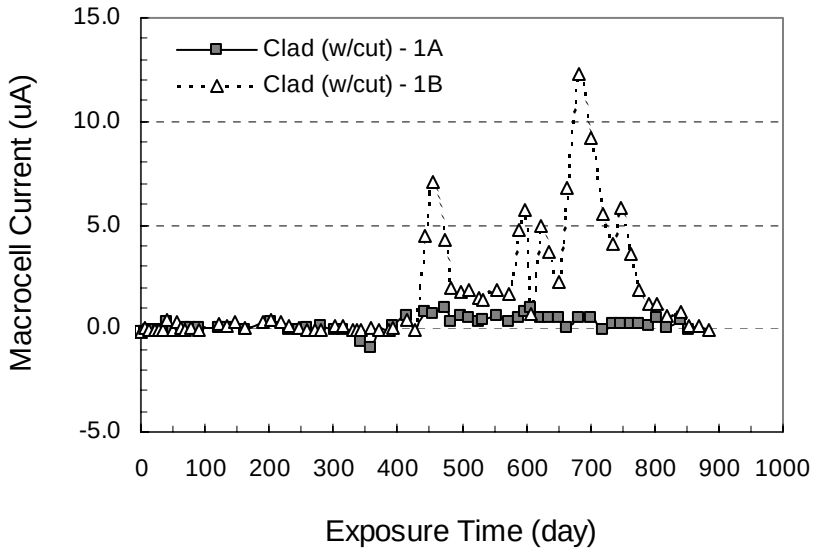

Figure 10. The macrocell currents flowing between clad bars with cuts 1A and 1B and their respective accompanying bottom clad bars.

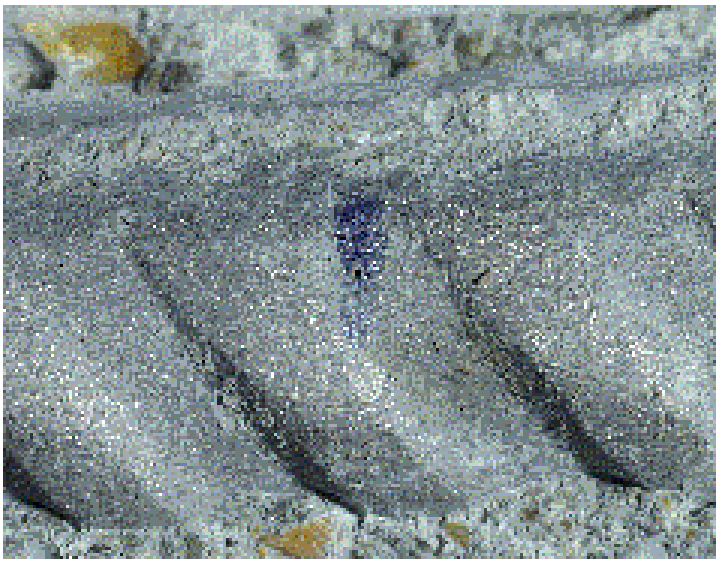

Figure 11. One of the holes (marked area in the center) drilled through the cladding of a clad bar. Notice the absence of any sign of corrosion around the hole, even though it was apparently not filled with cement paste.